Springer

Journal of Mechanical Science and Technology 22 (2008) 1993~1997

Journal of Mechanical Science and Technology

www.springerlink.com/content/1738-494x
DOI 10.1007/s12206-008-0744-7

Effects of centerline curvature and cross-sectional shape transitioning in the subsonic diffuser of the F-5 fighter jet †

I. H. Ibrahim[1], E. Y. K. Ng[1,*], K. Wong[2] and R. Gunasekaran[2]

[1]*School of Mechanical and Aerospace Engineering, Nanyang Technological University, 50 Nanyang Avenue, Singapore 639798*
[2]*Republic of Singapore Air Force (RSAF), Air Logistic Department, 506 Airport Road, Singapore 534395*

(Manuscript Received April 16, 2008; Revised June 25, 2008; Accepted July 23, 2008)

Abstract

Intake geometries result in unwanted secondary flows and formations of vortices which affect the engine performance. This paper investigates the effects of the curvature and cross-sectional shape transitioning of the actual F-5 duct. Two additional different geometries were set up to isolate each parameter; a circular cross-sectional duct with similar centerline configuration and a straight duct with similar cross-sectional transitioning as the F-5 duct. To measure the efficiency of duct flow, the distortion index (DC (60)) and pressure recovery are used. It is found that the straight duct with similar cross-sectional transitioning as the F-5 intake resulted in a 2.1% increase in pressure recovery and an 86% decrease in distortion when compared with the baseline intake. Also, the baseline intake resulted in a 0.5% increase in pressure recovery and a 15% decrease in distortion compared to the constant circular cross-sectional duct.

Keywords: S-duct; Curved diffuser; Cross-sectional shape; F-5; Distortion; Recovery

1. Introduction

The intake lies in a fore portion of the propulsion system in a plane. In the twin engine F-5 Fighter, each intake lies within the wing-root section of the aircraft. The placement and design of the intakes follows the contours of the main body of a fighter plane for external aerodynamic reasons. It is because of these reasons that a meandering shaped diffuser results. The curvature of an intake could result in unwanted secondary flows and formations of vortices which would inadvertently affect the engine performance and could result in flutter and stall. Within the intake, a multitude of ramp and bleed systems governed the airflow towards the boundary between the engine and the intake, known also as the Aerodynamic Interface Plane (AIP). To simplify this study, the geometry simulated investigates the intake solely without any integrated systems. The geometry focused is at the port side of the F-5 Fighter..

The simulation program that is built on and used in this research is COMSOL [1] [2]. The validation is initially done by comparing results of the S-duct [3]. Upon validation, similar boundary conditions are implemented into the F-5 duct. Taking the F-5 as the baseline configuration, two additional geometries are then set up. The two geometries isolate each parameter; a circular cross-sectional duct with similar centerline configuration to isolate cross-sectional shape change; and a straight duct with similar cross-sectional transitioning as the F-5 duct to isolate centerline curvature. Airflow efficiency is measured by comparing recovery and distortion factors.

2. Previous studies

The non-diffusing circular s-duct [3] was reproduced in the present paper. Contra-rotating vortices were found embedded in the lower part on the exit

† This paper was presented at the 9th Asian International Conference on Fluid Machinery (AICFM9), Jeju, Korea, October 16-19, 2007.

*Corresponding author. Tel.: +65 790 4455, Fax.: +65 791 1859
E-mail address: myknng@ntu.edu.sg

and expelled low-velocity fluid toward the center of the cross section. This phenomenon was also numerically obtained using a full 3-d Navier-Stokes equation [4, 5]. The analysis was solved with algebraic and two-equation turbulence models.

The issues of changing cross-sectional shape as well as centerline curvature were described in numerical simulation studies [6, 7]. Both geometries were similar with the present F-5 intake; an elliptical inlet that transcends to a circular exit. Two other geometries to isolate the factors of changing cross-sectional area and centerline curvature were set up. While centerline curvature in the baseline F-16 configuration is strong enough to produce secondary flow vortex, the changing cross-section shape suppresses its formation.

This present paper attempts to build on existing works of [6, 7]. Using the F-5 duct as geometry, pressure recoveries and distortion coefficient (DC) factors are introduced to quantify the effects of cross-sectional shape change and centerline curvature.

3. Governing equations

The present simulations have been performed using COMSOL, based on the finite elements approach [1]. Two turbulence models were used on the non-diffusing circular duct. Both the k-ε [1] and k-Ω [2] physics settings are modeled using the General form. Constant enthalpy was assumed to exist in the duct and hence the energy equation was not included.

Written in COMSOL environment, the Navier-Stokes equations are shown below:

Momentum equation:

$$\rho u \cdot \nabla u = -\nabla p + \nabla \cdot \left[(\eta + \eta_T)\left(\nabla u + (\nabla u)^T\right)\right] \left(-(2/3)(\nabla \cdot u) I\right) + F \quad (1)$$

where ρ is density, u is the axial velocity of the duct, p is static pressure, η is the dynamic viscosity η_T is the turbulent viscosity and F is force per unit volume

Continuity equation:

$$\nabla \cdot (\rho u) = 0 \quad (2)$$

The k-ε and k- Ω turbulence energy and dissipation equations are derived and explained in [1] and [2]. The constants used suited in their standard forms.

4. Boundary conditions

The CFD simulations for the circular S-duct as well as the F-5 intake were conducted with a uniform velocity of 0.6 Mach. The symmetry of the S-duct allowed for a slip condition to exist at the symmetrical plane. This condition was however not present for the F-5. A neutral boundary condition was thus specified as the outlet condition for both ducts. This results in a zero gauge pressure condition present at the outlet. The turbulent quantities are defined using the turbulent kinetic energy and dissipation rate, further explained in [1] and [2].

5. Measurements for total pressure coefficient, pressure recovery and distortion coefficient (DC)

The total pressure coefficient used in the intake stations is measured by:

$$\text{Total pressure coefficient} = (P_{\text{total, local}} - P_{\text{static, inlet boundary}}) / (P_{\text{dynamic}}) \quad (3)$$

Both pressure recovery and DC (60) values are taken at the AIP datum.

6. Results and discussion

6.1 Circular S-duct

The dimensions of the non-diffusing circular s-duct [3] are shown in Fig. 1. The inlet speed is chosen at Mach 0.6, resulting in a Reynolds number of 1.76 x 10^6 with respect to the inlet diameter. These values are used to replicate the similar experimental conditions.

Convergence test are carried out to identify the suitable number of elements required. The number of

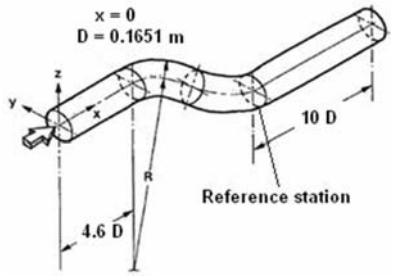

Fig. 1. The circular S-duct geometry used for validation analysis. R, the radius of curvature, is 32.5 inches, or 0.8255 m.

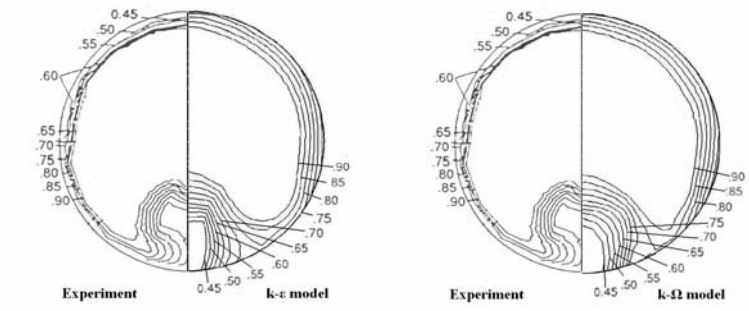

Fig. 2. Total pressure contours comparison between experimental and k-ε and k-Ω results respectively at the reference station.

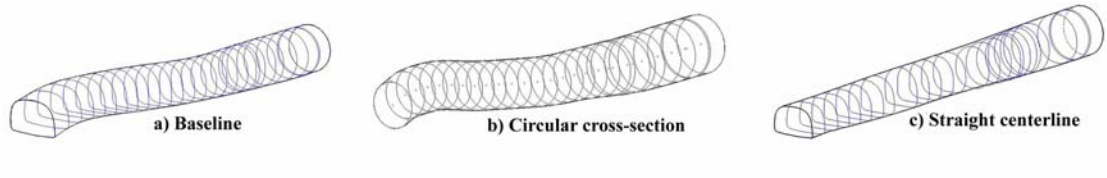

Fig. 3. a) Baseline configuration, b) Circular cross-section configuration c) Straight centerline configuration.

elements where solution is independent of mesh density is found to be approximately 2473, resulting about 23188 degrees of freedom. The meshing quality was kept above 0.3 so that the solution resulted would not be affected. Denser mesh was also fitted near the wall boundaries to adequately capture boundary layer separation. This resulted in y^+ values between 30 and 300.

The high number of degrees of freedom requires an iterative solver for convergence. The Flexible Generalized Minimum Residual (FGMRES) solver with VANKA preconditioner is chosen. A relative tolerance of 10 E-6 is chosen for linear iterations and the number for iterations is limited to 10000. The iterations terminate when the relative preconditioned residual is less than the required tolerance divided by a factor, which is set under the error estimate factor of 400. Finally, the number of restarts for the solver to perform is limited to 50. This is number of iterations the solver does to achieve the desired convergence criteria, before a restart to the initial condition. The k-ε and k-Ω simulations were carried out on a Pentium IV PC, consuming about 30 and 35 minutes of the net CPU time per run respectively.

Results are compared by taking total pressure contours at reference station downstream of the duct as indicated in Fig. 1. Simulations for COMSOL and experimental results are plotted in Fig. 2.

Based from the experimental results, the final station (the station at the end of the second bend), formation of low total-pressure flow could be seen at the outer portion of the bends. This formation is attributed to the difference in static pressure gradients that existed in both the first and second bend, pushing the low velocity fluid towards the core similar to experimental results obtained [3].

From the comparison of results, it can be seen that both the k-ε and k-Ω models showed good agreement with the experimental data. The size of the core flow as well as vortex formation matched reasonably to that obtained by experimental data. The shape of the core flow obtained by the k-Ω model provided slightly better accuracy, as seen at the curvature of the core flow as well as the resultant vortex formation.

6.2 Effects of centerline curvature and change in cross-section shape

The k-Ω model was then used to simulate in the F-5 intake and two additional geometries to investigate the effects of curvature and cross sectional transitioning (Fig. 3). The first was the baseline F-5 intake (Fig. 3a). The second geometry had the same centerline shape and area distribution as the baseline configuration, but with circular cross-sections (Fig. 3b). The third has the same cross-section shape and area distribution as the baseline configuration, but with a straight centerline (Fig. 3c).

Similar meshing as well as solver settings was used for the F-5 duct geometry. A total of 4134 elements

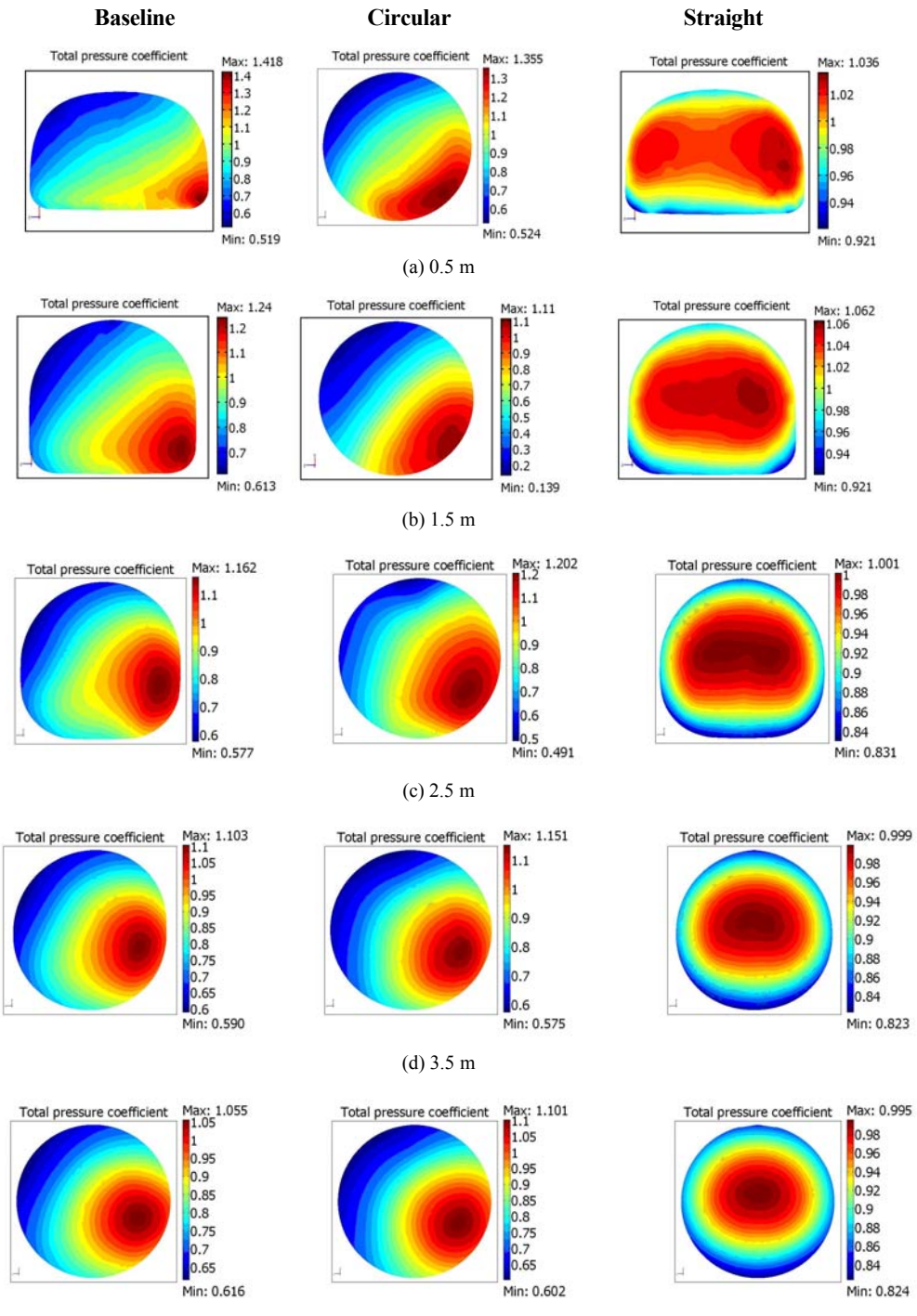

Fig. 4. The baseline duct shows the total pressure contours analysis of the F-5 port side duct solved by the k-Ω model. The outlet boundary indicates non-axis symmetry character, an undesirable compressor intake feature. Proper orientation of the duct with respect to normal flight will mean that the above views will have to be rotated 90º clockwise. The circular duct with similar centerline shape (centre) showed similar profile shapes as the baseline configuration (left). The straight duct with similar cross-sectional shape (right) as the baseline configuration showed better symmetry and pressure recovery.

Table 1. Predicted pressure recoveries and distortion coefficients of the three ducts.

Duct type	DOF	CPU Time (seconds)	Pressure recovery	DC(60)
F-5	37750	4206	0.973	0.33
Circular	32846	2318	0.968	0.38
Straight centerline	36936	4095	0.994	0.045

were used (with grid invariant test) to generate approximately 37750 degrees of freedom. Computation time took approximately 1.2 hours of the net CPU time per run.

Regions of low total pressure were present at the top left side of the F-5 baseline duct, and this character remained unchanged throughout. At the outlet boundary (4.5 m, Fig. 4(e)), it can be seen that there is a non-axis symmetry formation. This high total pressure distortion is undesirable for the intakes of engines.

The total pressure coefficient for the circular cross-section duct with similar centerline shape is virtually identical to that obtained by the baseline configuration. The region of high total pressure persists at the bottom right side of the duct as obtained by the baseline configuration. However, pressure recovery is lower than that compared to the baseline configuration.

For the straight centerline configuration, results show a significant difference from the baseline and circular configurations. The total pressure profiles throughout the duct are symmetrical. Pressure recovery is also notably greater in the straight centerline configuration as one is expecting. This is seen in the higher ranges of maximum and minimum total pressure values.

Distortion coefficient and pressure recovery values are given in Table 1. Compared to F-5 duct baseline values, it can be seen that the straight centerline duct resulted in the best pressure recovery and lowest distortion.

In all, changing the cross-sectional shape of the baseline duct to fully circular will result in a decrease in pressure recovery of 0.5% and an increase of 15% in distortion coefficient. Changing the centerline curvature into a straight duct would result in an increase of pressure recovery of 2.1% and a decrease in distortion coefficient of 86%.

7. Conclusion

The following remarks are observed:

1) The k-Ω turbulent model provided a slightly more accurate result as compared to the k-ε model for the circular s-duct by visually inspecting the characteristics of core flow and the vortex formation at the outlet of the non-diffusing duct.

2) The observations confirmed the initial hypothesis and show that both cross-sectional shape changes and centerline curvature play a role in the outcome of the air flow profile. A straight-line configuration produces the best pressure recovery and distortion coefficient.

Further studies can be enhanced by putting the calculation losses in tandem with the results of distortion flow through the compressor and engine face to give an overall view of the intake propulsion of a fighter plane.

Acknowledgements

The authors would like to thank HQ RSAF for permission to publish this work together with the data support.

References

[1] COMSOL Multiphysics 3.2, Chemical engineering module user's guide, Chapter 4, Turbulent Flow section, (2005).

[2] COMSOL Multiphysics 3.3, Release Notes, January 2007, Chapter 1, COMSOL 3.3a Release Notes, 55-57.

[3] A. D. Vakili, J. M. Wu and M. K. Bhat, 1986, Experimental Investigation of Secondary Flows in a Diffusing S-Duct, University Of Tennessee, Space Inst. TR UTSI 86/14, Nashville, TN.

[4] G. J. Harloff, C. F. Smith, J. E. Bruns and J. R. DeBonis, April 1992, Three-Dimensional Compressible Turbulent Computations for a Diffusing S-Duct, NASA Contractor Report 4392.

[5] G. J. Harloff, C. F. Smith, J. E. Bruns and J. R. DeBonis, Navier-stokes analysis of three-dimensional S-ducts, *Journal of Aircraft*, 30 (4) (1993) 526-533.

[6] L. A. Povinelli and C. E. Towne, Viscous analyses for flow through subsonic and supersonic intakes. NASA Technical Memorandum E-3209, Lewis Research Center, Cleveland, Ohio (1986).

[7] C. E. Towne and B. H. Anderson, 1981, Numerical simulation of flows in curved diffusers with cross-sectional transitioning using a three dimensional viscous analysis, *AIAA Paper 81-0003 (Also NASA TM-81672).*